OPEN REPORT
SCK•CEN-BLG-1057

Influence of Striking Edge Radius (2 mm versus 8 mm) on Instrumented Charpy Data and Absorbed Energies

Work performed during a 3-month secondment at NIST, Boulder CO (USA), June-August 2008

Enrico Lucon

August, 2008

SCK•CEN
Boeretang 200
BE-2400 Mol
Belgium

OPEN REPORT OF THE BELGIAN NUCLEAR RESEARCH CENTRE
SCK•CEN-BLG-1057

Influence of Striking Edge Radius (2 mm versus 8 mm) on Instrumented Charpy Data and Absorbed Energies

Work performed during a 3-month secondment at NIST, Boulder CO (USA), June-August 2008

Enrico Lucon

August, 2008
Status: Unclassified
ISSN 1379-2407

SCK•CEN
Boeretang 200
BE-2400 Mol
Belgium

Distribution List

R. Chaouadi	NMS, SCK•CEN	1
E. Lucon	NMS, SCK•CEN	1
J.-L. Puzzolante	NMS, SCK•CEN	1
J. Schuurmans	NMS, SCK•CEN	1
M. Scibetta	NMS, SCK•CEN	1
S. Van Dyck	NMS, SCK•CEN	1
R. Gérard	SUEZ-Tractebel	1
	Secretariaat NMS	3

Studiecentrum voor Kernenergie
Centre d'étude de l'énergie Nucléaire
Boeretang 200
BE-2400 Mol
Belgium

Phone +32 14 33 21 11
Fax +32 14 31 50 21

http://www.sckcen.be

Contact:
Knowledge Centre
library@sckcen.be

Preface

This work was performed during my secondment at NIST (National Institute of Standards and Technology) in Boulder, Colorado (USA), between June and August 2008.

An abridged version of this report was submitted to International Journal of Fracture for publication on 15 August 2008.

Abstract

The most commonly used test standards for performing Charpy impact tests (ISO 148 and ASTM E 23) envisage the use of strikers having different radii of the striking edge, i.e. 2 mm (ISO) and 8 mm (ASTM). The effect of striker geometry on Charpy results was extensively studied in the past in terms of absorbed energy measured by the machine encoder, but few investigations are available on the influence of striker configuration on the results of instrumented Charpy tests (characteristic forces, displacements and integrated energy). In this paper, these effects are investigated based on the analysis of published results from three interlaboratory studies and some unpublished Charpy data obtained at SCK•CEN. The *t*-test was used for establishing the statistical significance of the observed effects. The instrumented variables which are the most sensitive to the radius of the striking edge are the maximum force and its corresponding displacement, with 8mm-strikers providing systematically higher values. The effect on general yield forces, on the other hand, is less consistent and more difficult to rationalize, although 2mm-strikers generally tend to deliver higher values. Absorbed energies, obtained both from the instrumented trace and from the pendulum encoder, are almost insensitive to the type of striker up to 200 J. For higher energy levels, the values obtained from 8mm-strikers become progressively larger. Data scatter is generally higher for 2mm-strikers.

Keywords

Instrumented Charpy tests; striker configuration; absorbed energy; t-test.

Table of Contents

1 Introduction

Impact testing has a history extending back to the 1850's (Siewert et al. 2000), when engineers realized that loading rate can significantly affect material properties. For structural steels, the main result of increasing loading rate is to raise the yield and tensile strength, which in turn causes a decrease in cleavage fracture toughness, an increase in ductile fracture toughness and a shift in the ductile-to-brittle transition temperature. Loading rate must be therefore be considered when designing structures subject to dynamic loading (e.g. earthquakes), ships and road vehicles in collision, aircraft landing gear and, at the highest rates, for projectile or armor ballistics and explosive shock.

The simplest mechanical test that can be conducted to characterize the fracture resistance of metallic materials at dynamic loading rates is the Charpy impact test, which has recently celebrated its first centennial (ASTM 2000; ESIS 2002). Nowadays, there are two main test standards that regulate worldwide the performance of Charpy impact tests and the maintenance of test machines: ASTM E 23 (current version 2007) and ISO 148 (current version 2006).

The two test standards are fairly similar, but one of the most significant differences relates to the configuration of the pendulum striker which impacts the specimen. Although both strikers have an angle of 30°, the striker prescribed by ISO 148 is thinner and has a radius of 2 mm for the leading edge, whereas the ASTM striker has an 8 mm radius and in addition features two relatively sharp edges where the nose radius meets the sides of the striker (Fig. 1).

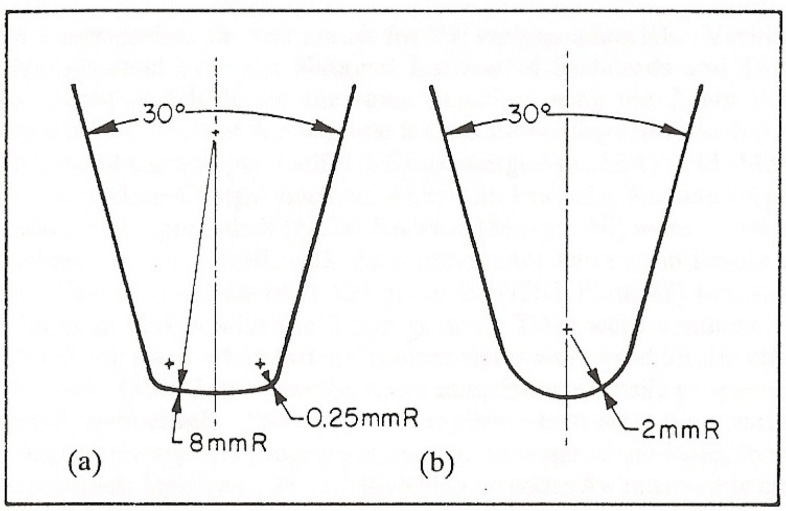

Fig. 1 Schematic drawing of the (a) ASTM (8 mm radius) and (b) ISO (2 mm radius) striker.

Numerous published studies (Towers 1983; Revise 1990; Fink 1990; Naniwa et al.1990; Ruth 1995; Nanstad and Sokolov 1995; Tanaka et al. 1995; Siewert and Vigliotti 1995; McCowan et al. 2000) have investigated the effect of the striking edge radius on the results of "conventional" (i.e. non-instrumented) Charpy tests, in terms of absorbed energy KV, lateral expansion and shear fracture appearance.

For absorbed energy, differences between the two strikers are small (within experimental uncertainties) below a given threshold energy, which was reported by most authors to be around 200 J (Ruth 1995; Naniwa et al. 1995; McCowan et al 2000). However, values as low as 60 J (Towers 1983; Morita and Kobayashi 2004) or 100 J (Siewert and Vigliotti 1995) were also reported for some materials. This threshold appears to be material-dependent (Nanstad and

Sokolov, 1995) and related to the characteristic fracture properties of the material (Tanaka et al. 1995).

Above this threshold value, specimens tested with an 8mm-striker were shown to deliver significantly higher absorbed energies than those tested with a 2 mm-striker. The main reasons for this increase in KV, often observed when test specimens do not separate, were identified in the interaction between the specimen and the 8mm-striker corners and in the increased friction between specimen and anvils (Tanaka et al. 1995). In additional, the standard deviation of results was also reported to be significantly larger for the 2mm-striker (Siewert and Vigliotti 1995).

Below the threshold, the general consensus is that the two strikers are equivalent, although marginally higher values for 2mm-strikers were reported around 16 J (Ruth 1995) and at higher energies (McCowan et al 2000); on the other side, Fink (1990) proposed a linear correlation:

$$KV_{2mm} = 1.042 KV_{8mm} + 0.70 \tag{1}$$

implying that up to 200 J, 2mm-strikers yield 4% higher energy than 8mm-strikers.

As far as other Charpy parameters are concerned, most authors agree that lateral expansion values from 2mm-strikers are generally higher, whereas no differences can be observed in terms of shear fracture appearance (Naniwa et al. 1990; Nanstad and Sokolov 1995; McCowan et al 2000).

Limited information, and mostly of qualitative rather than quantitative nature, is available in the literature on the effect of striking edge radius on instrumented Charpy data (Naniwa et al. 1990; Nanstad and Sokolov 1995; Tanaka et al. 1995; Morita and Kobayashi 2004).

Instrumented Charpy tests, originally developed in the early 1920's (Manahan and Siewert, 2006) are currently regulated by test standard ISO 14556, while standardization is also in progress within the ASTM E28.07 subcommittee.

A well-known effect of striker configuration, which is clearly visible on the instrumented traces of highly ductile materials tested with an 8mm-striker, is the characteristic "bump" (also referred to as "tail") that is observed at the end of the test records, just before the force comes back to the baseline (Fig. 2). This feature, which is absent in tests performed using a 2mm-striker, is caused by the interaction between the heavily deformed specimens and the corners of the 8mm-striker just before the sample is released (Schuurmans et al. 2008). It is considered to be one of the main contributions to the large difference between strikers at high energy levels, together with the increased friction between specimen and anvils (Naniwa et al.1990; Ruth 1995; Nanstad and Sokolov 1995; Tanaka et al. 1995; Siewert and Vigliotti 1995; McCowan et al. 2000).

This paper focuses on the influence of striker configuration (2 mm vs. 8 mm) on the results of instrumented Charpy tests, namely characteristic forces (F_{gy}, force at general yield; F_m, maximum force), characteristic displacement at maximum force (s_m) and instrumented total energy (W_t, calculated by integrating the force/displacement test record). Absorbed energy values KV were also included in the evaluations, in order to obtain comparisons with the available literature as summarized above.

To this aim, results from several international round-robin exercises were analyzed, in which participants used instrumented strikers conforming to either ASTM E 23 or ISO 148/ISO 14556. Additional information was derived from instrumented Charpy data obtained at SCK•CEN using both 2mm and 8mm instrumented strikers installed.

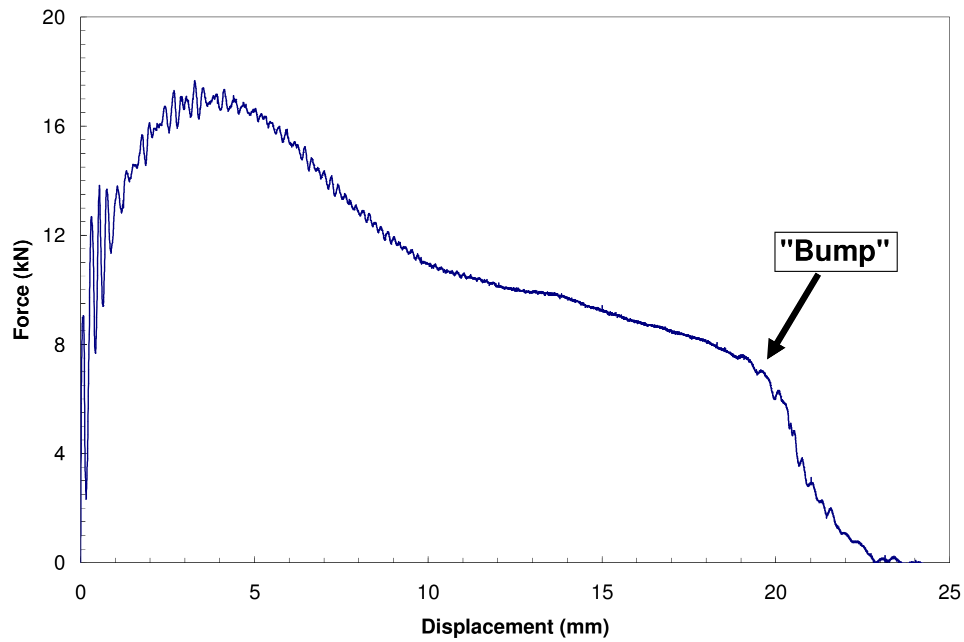

Fig. 2 Example of instrumented record for a highly ductile specimen (KV = 260 J) tested with an 8mm-striker.

2 Analytical approach and data sets considered

Instrumented Charpy data from three interlaboratory studies (ILS) were analyzed (Table 1). In these round-robins, laboratories from all over the world tested steel Charpy specimens using 2mm or 8mm instrumented strikers. More details on each ILS will be given below.

Table 1 Interlaboratory studies considered in this investigation.

Round-Robin	Period	No of materials tested	No of tests with 2mm-striker	No of tests with 8mm-striker
ASTM E28.07	1997-98	4	68	106
NIST	2006-07	2	99	60
IAEA CRP-8	2007	1	10	8
TOTAL		7	177	174

The ASTM E28.07 round-robin also included tests on the same 4 materials using sub size Charpy specimens with reduced "half-size" geometry (width and thickness 4.83 mm; length 24.13 mm; notch depth 0.97 mm). Participants used 2mm-strikers (89 tests) and scaled 8mm-strikers (striking edge radius = 3.96 mm; 36 tests). These data were also included in the analyses.

In addition, SCK•CEN performed instrumented Charpy tests, mainly on European reference materials, using the same test machine but two different strikers (2mm and 8mm). For one material (DIN 22NiMoCr37 pressure vessel steel), tests were performed at different temperatures.

For each data set and each instrumented Charpy parameter, mean values and standard deviations were calculated and compared for 2mm and 8mm strikers. In order to assess how significant is the effect of striker configuration, the differences between calculated mean values were analyzed by means of a simple statistical test (unpaired *t*-test). The degree of statistical significance depends on the value of the two-tailed probability[1] P using a threshold value 0.05 (95% confidence level), as follows:

- $P > 0.05 \Rightarrow$ not significant
- $0.01 < P < 0.05 \Rightarrow$ significant
- $0.001 < P < 0.01 \Rightarrow$ very significant
- $P < 0.001 \Rightarrow$ extremely significant.

3 Interlaboratory studies

3.1 ASTM E28.07 round-robin (1997-98)

To promote the development of a new ASTM test standard for instrumented impact testing of full-size and sub size Charpy specimens, Task Group E28.07.08 launched a round-robin exercise involving 8 laboratories (6 from Europe and 2 from the US) (Manahan et al. 2000). Three labs used a 2mm-striker and five used an 8mm-striker. Three materials were tested: A533B cl.1 (at room temperature and 150°C) and two NIST certified reference materials (CRM) of different energy levels (low and high).

Table 2 shows mean values and standard deviations for the test results and the outcome of the *t*-test for the statistical significance of the difference between strikers at the 95% confidence level.

Table 2 Analysis of the results of the ASTM E28.07 round-robin (full-size specimens).

Parameter		A533B (RT)			A533B (150°C)			Low energy CRM			High energy CRM		
		2mm	8mm	Δ	2mm	8mm	Δ	2mm	8mm	Δ	2mm	8mm	Δ
F_{gy} (kN)	N	17	29		17	30		N/A[2]			17	30	
	Mean	**13.76**	**12.51**	>>	**12.03**	**10.55**	>>>				**21.37**	**19.11**	>>>
	SD	1.325	1.134		0.554	0.835					1.213	1.545	
F_m (kN)	N	17	29		17	30		17	17		17	30	
	Mean	**18.16**	**19.06**	<<<	**16.14**	**17.33**	<<<	**34.55**	**33.84**	~	**24.59**	**24.93**	~
	SD	0.731	0.413		0.295	0.335		1.303	1.854		0.644	0.525	
s_m (mm)	N	11	29		11	28		11	11		11	22	
	Mean	**2.70**	**3.16**	<<<	**3.24**	**3.52**	<<	**0.85**	**0.91**	<<	**1.41**	**1.90**	<<<
	SD	0.287	0.212		0.261	0.265		0.055	0.059		0.212	0.042	
W_t (J)	N	17	29		17	28		17	17		17	28	
	Mean	**79.94**	**76.66**	~	**130.02**	**130.76**	~	**23.67**	**24.31**	~	**121.22**	**117.74**	~
	SD	20.935	15.731		5.792	5.673		2.963	2.149		7.691	6.612	
KV (J)	N	17	29		17	28		17	17		17	28	
	Mean	**80.91**	**76.69**	~	**128.81**	**130.30**	~	**24.52**	**24.36**	~	**119.72**	**117.51**	~
	SD	20.396	15.666		4.869	5.363		1.555	1.827		7.262	1.307	

LEGEND N = number of available data; SD = standard deviation; Δ = statistical significance of the difference between mean values (*t*-test):

~ : 2 mm ≈ 8 mm (difference not significant)
> : 2 mm > 8 mm (difference significant)
>> : 2 mm > 8 mm (difference very significant)
>>> **:** 2 mm > 8 mm (difference extremely significant)
< : 2 mm < 8 mm (difference significant)
<< : 2 mm < 8 mm (difference very significant)
<<< **:** 2 mm < 8 mm (difference extremely significant)

[1]In statistical hypothesis testing, P is the probability of obtaining a value of the test statistic at least as extreme as the one that was actually observed, given that the null hypothesis (i.e. no difference between the means) is true.
[2]F_{gy} values are not considered in the case of fully brittle specimens, since general yield does not occur or cannot be unambiguously defined.

The same analyses are presented in Table 3, but for sub size specimens and considering strikers having 2 mm or 4 mm (nominally 3.96 mm) radius.

Table 3 Analysis of the results of the ASTM E28.07 round-robin (sub-size specimens).

Parameter		A533B (RT)			A533B (150°C)			Low energy CRM			High energy CRM		
		2mm	4mm	Δ	2mm	4mm	Δ	2mm	4mm	Δ	2mm	4mm	Δ
F_{gy} (kN)	N	22	6		22	12		N/A			23	12	
	Mean	**2.84**	**2.47**	>	**2.50**	**2.68**	<<<				**3.64**	**3.55**	~
	SD	0.344	0.205		0.074	0.219					0.601	0.215	
F_m (kN)	N	22	6		22	12		22	6		23	12	
	Mean	**3.65**	**4.19**	<<<	**3.32**	**3.53**	<<<	**4.70**	**5.59**	<<<	**4.67**	**5.24**	<<<
	SD	0.087	0.109		0.068	0.167		0.161	0.179		0.150	0.290	
s_m (mm)	N	16	6		16	12		16	6		17	12	
	Mean	**1.19**	**1.01**	>>>	**1.39**	**1.32**	>	**0.74**	**0.82**	<<	**0.74**	**0.81**	<<<
	SD	0.068	0.016		0.112	0.054		0.036	0.087		0.038	0.042	
W_t (J)	N	22	6		22	12		22	6		23	12	
	Mean	**10.89**	**11.53**	~	**10.88**	**11.19**	~	**10.55**	**11.55**	<<	**10.59**	**11.24**	~
	SD	0.735	0.454		0.487	0.636		0.840	0.167		0.821	6.612	
KV (J)	N	22	N/A	N/A	22	6		22	N/A	N/A	23	6	
	Mean	**11.10**			**10.99**	**10.73**	~	**10.94**			**10.96**	**10.84**	~
	SD	0.793			0.420	0.231		0.373			0.353	0.177	

3.2 NIST round-robin (2006-07)

The NIST round-robin exercise (McCowan et al. 2008) used certified reference materials from two energy levels, low energy (~ 20 J) and high energy (~ 110 J). The exercise involved 8 laboratories, 7 from Europe and 1 from the US, who tested 10 full-size specimens of each energy level at room temperature (RT); some laboratories tested multiple series of specimens, using the same machine or different machines. The results and the outcome of the statistical analyses are given in Table 4.

Table 4 Analysis of the results of the NIST round-robin.

Parameter		Low energy level			High energy level		
		2mm	8mm	Δ	2mm	8mm	Δ
F_{gy} (kN)	N	N/A			39	30	
	Mean				**18.96**	**20.31**	<<<
	SD				1.055	0.342	
F_m (kN)	N	50	30		49	30	
	Mean	**32.34**	**34.16**	<<<	**23.80**	**24.63**	<<<
	SD	1.553	1.865		0.662	0.306	
W_t (J)	N	40	30		49	30	
	Mean	**18.74**	**18.43**	~	**109.88**	**105.76**	>>>
	SD	1.581	0.571		3.578	3.060	
KV (J)	N	50	30		49	30	
	Mean	**20.53**	**19.04**	>>>	**109.30**	**108.84**	~
	SD	1.437	0.877		2.229	2.903	

3.3 IAEA CRP8 (2007)

The Coordinated Research Project n°8 (CRP8) of the International Atomic Energy Agency (IAEA) was titled "Master Curve Approach to Monitor Fracture Toughness of RPV

Steels: Effects of Bias, Constraint, and Geometry" (Kang 2007). One of its Topic Areas dealt with loading rate effects on Master Curve (Viehrig and Lucon 2007), and included an interlaboratory comparison of instrumented Charpy test results among 9 laboratories (5 from Europe, 2 from the US, 1 from Japan and 1 from Korea). Each participant tested at room temperature 2 full-size specimens of the high energy European Reference Material (ERM, ~ 150 J). Test results and statistical analyses are shown in Table 5.

Table 5 Analysis of the results of the IAEA CRP8 interlaboratory comparison.

Parameter		High energy ERM		
		2mm	8mm	Δ
F_{gy} (kN)	N	10	8	
	Mean	**17.81**	**19.18**	<
	SD	1.270	0.488	
F_m (kN)	N	10	8	
	Mean	**23.21**	**24.92**	>
	SD	1.911	1.137	
W_t (J)	N	10	8	
	Mean	**149.57**	**143.08**	~
	SD	13.43	6.071	
KV (J)	N	10	8	
	Mean	**151.61**	**142.24**	>>
	SD	5.027	6.377	

4 SCK•CEN data

4.1 Instrumented Charpy tests on ERM specimens

European reference Charpy specimens of two energy levels (low and medium – approximately 25 J and 80 J respectively) were tested at RT at SCK•CEN using two pendulum machines. On each machine, two instrumented strikers were used, one conforming to the ASTM (8 mm) and one to the ISO (2 mm) design. These data, unlike the round-robin results previously analyzed, allow isolating the influence of striker configuration from any additional effect caused by the use of machines having different characteristics such as pendulum design, mass, capacity, speed, hammer type (C-type or U-type) etc. Unfortunately, the number of available data is limited.

The analyses are summarized in Table 8.

Table 8 Analysis of the results of ERM specimens tested at SCK•CEN.

Parameter		ERM low energy (batch 1-30-E11)			ERM low energy (batch 1-AF-30)			ERM medium energy		
		2mm	8mm	Δ	2mm	8mm	Δ	2mm	8mm	Δ
F_{gy} (kN)	N	N/A			N/A			2	2	
	Mean							**24.05**	**23.46**	~
	SD							0.071	0.505	
F_m (kN)	N	4	5		5	4		2	2	
	Mean	**31.76**	**33.28**	<<	**34.04**	**33.21**	~	**27.58**	**29.12**	<
	SD	0.498	0.359		0.493	1.089		0.248	0.219	
s_m (mm)	N	4	5		5	4		2	2	
	Mean	**1.01**	**1.03**	~	**0.87**	**0.99**	<<<	**1.05**	**1.37**	~
	SD	0.035	0.015		0.020	0.019		0.142	0.131	
W_t (J)	N	4	5		5	4		2	2	
	Mean	**22.81**	**24.05**	~	**26.94**	**23.77**	>>>	**76.98**	**78.41**	~
	SD	0.991	0.610		0.362	0.242		0.367	3.578	

Parameter		ERM low energy (batch 1-30-E11)			ERM low energy (batch 1-AF-30)			ERM medium energy		
		2mm	8mm	Δ	2mm	8mm	Δ	2mm	8mm	Δ
KV (J)	N	4	5		5	4		2	2	
	Mean	**24.62**	**26.08**	~	**28.89**	**26.50**	>>	**80.10**	**78.20**	~
	SD	1.409	0.610		0.711	0.590		1.846	3.394	

4.2 Tests at different temperatures

Charpy specimens of a German ferritic pressure vessel steel, DIN 22NiMoCr37 (Heerens and Hellmann 2002), were tested using one test machine and two different instrumented strikers (2mm - 4 tests, and 8mm - 13 tests). Tests were run at different temperatures spanning the whole transition range from brittle to ductile behavior. Results obtained are shown in Fig. 3 (F_{gy}), Fig. 4 (F_m), Fig. 5 (s_m), Fig. 6 (W_t), Fig. 7 (KV), Fig. 8 (lateral expansion) and Fig. 9 (shear fracture appearance, SFA).

These results are particularly valuable since they provide the only absorbed energy data analyzed in this paper that exceed 200 J (at least in the upper shelf regime), as well as the only comparative information on lateral expansion (Fig. 8) and SFA (Fig. 9). The upper shelf energy (USE) ratio measured using the 2mm and the 8mm striker is 0.88 for W_t (Fig. 6) and 0.87 for KV (Fig. 7).

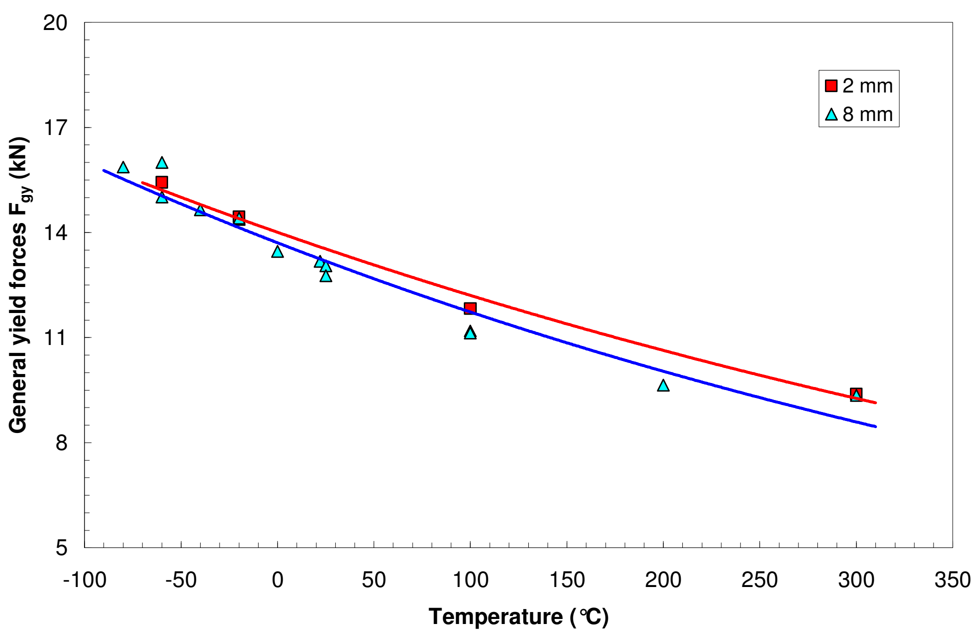

Fig. 3 Forces at general yield measured on 22NiMoCr37 using a 2mm and an 8mm-striker. Data are fitted by second-order polynomials.

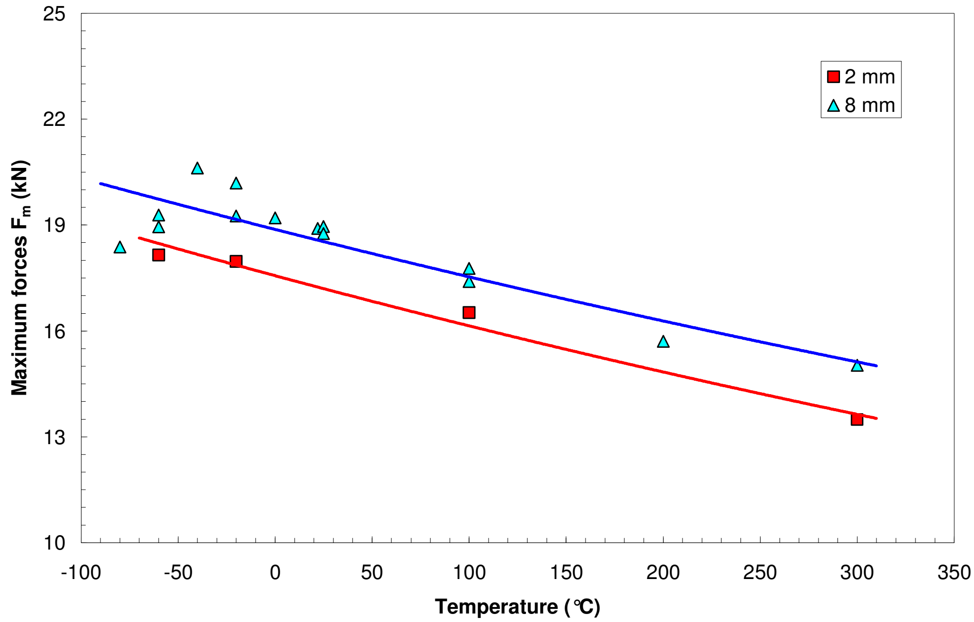

Fig. 4 Maximum forces measured on 22NiMoCr37 using a 2mm and an 8mm-striker. Data are fitted by second-order polynomials.

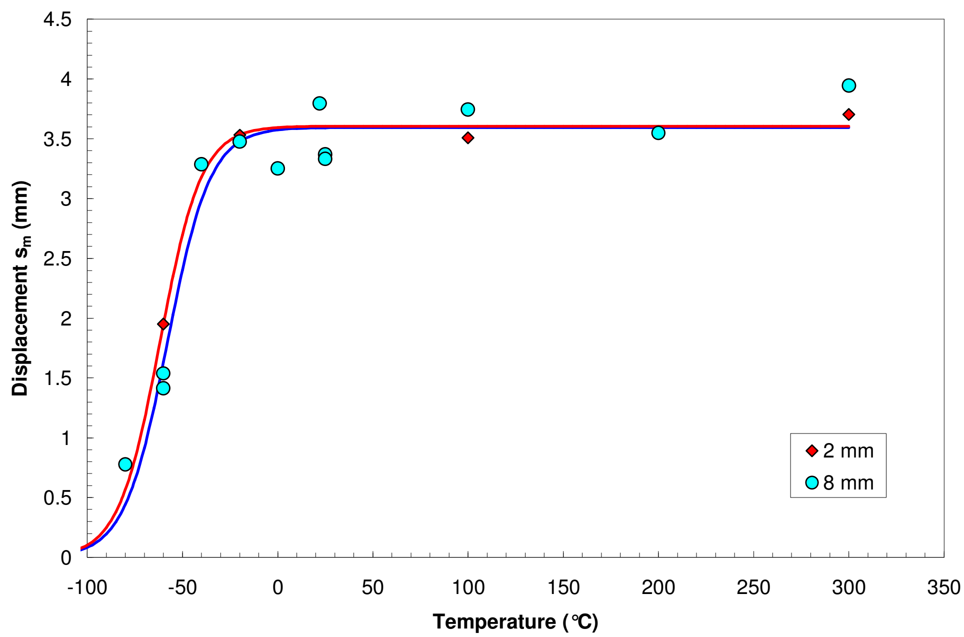

Fig. 5 Displacements at maximum force measured on 22NiMoCr37 using a 2mm and an 8mm-striker. Data are fitted by hyperbolic tangent curves.

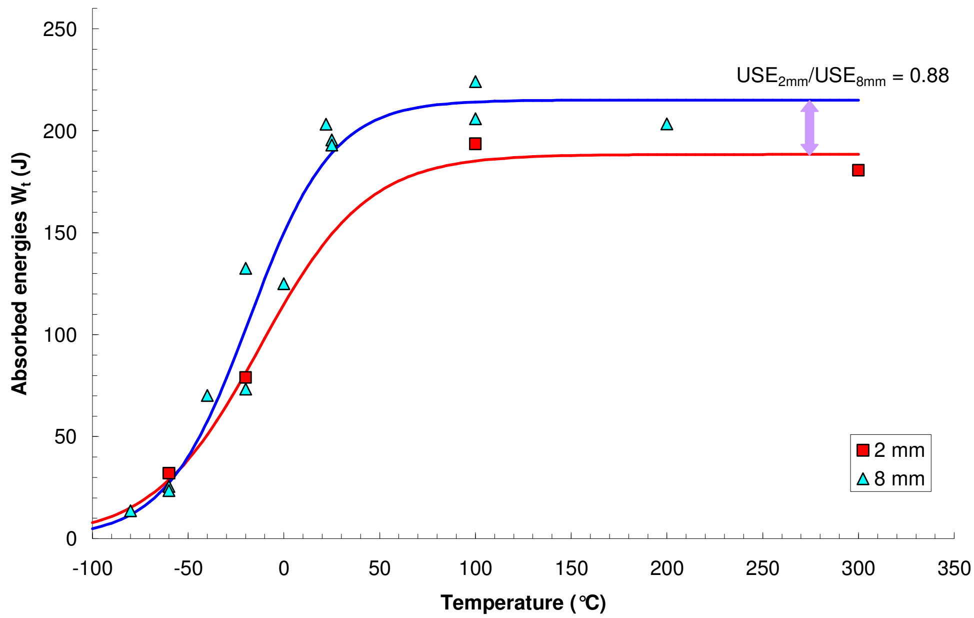

Fig. 6 Calculated absorbed energies measured on 22NiMoCr37 using a 2mm and an 8mm-striker. Data are fitted by hyperbolic tangent curves.

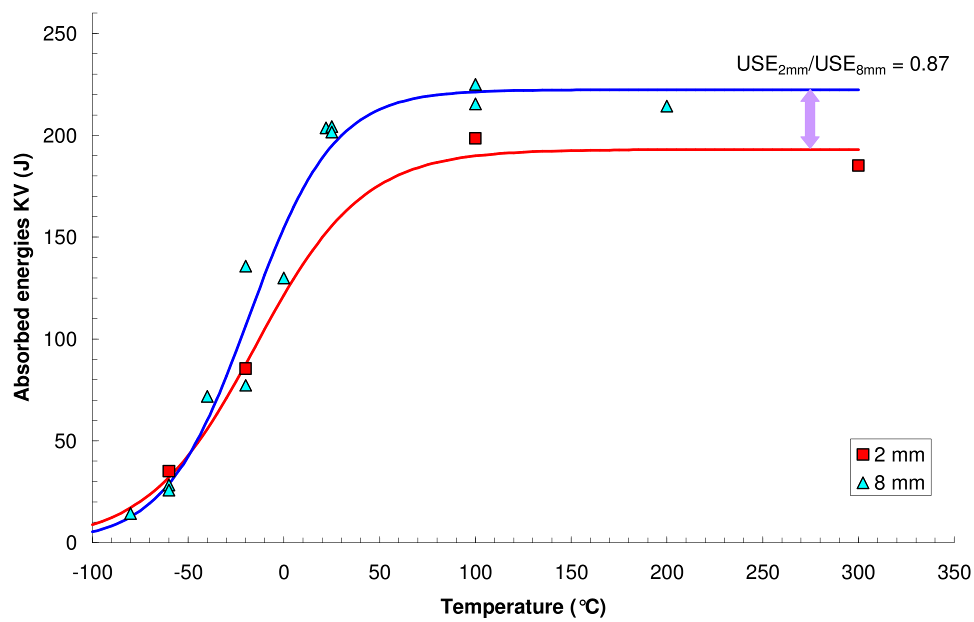

Fig. 7 Encoder absorbed energies measured on 22NiMoCr37 using a 2mm and an 8mm-striker. Data are fitted by hyperbolic tangent curves.

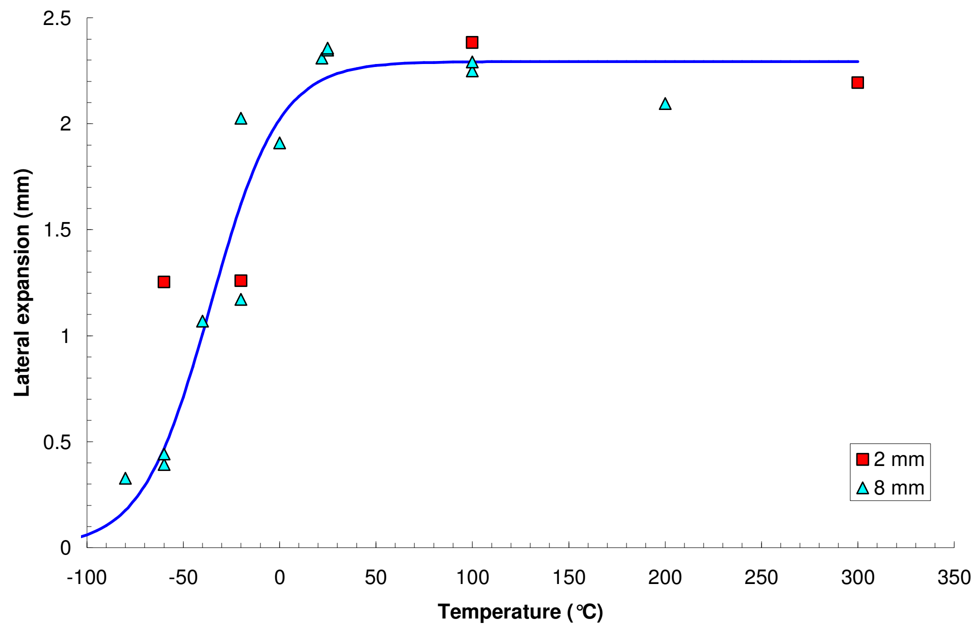

Fig. 8 Lateral expansion values measured on 22NiMoCr37 using a 2mm and an 8mm-striker. 8mm data are fitted by a hyperbolic tangent curve; 2mm data cannot be fit in a meaningful way.

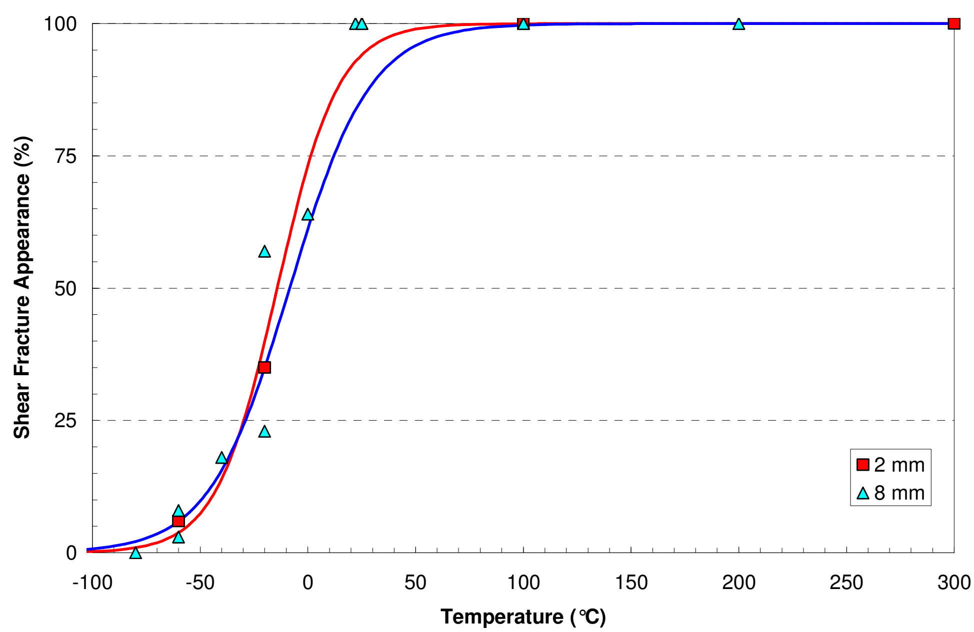

Fig. 9 Shear fracture appearance measured on 22NiMoCr37 using a 2mm and an 8mm-striker. Data are fitted by hyperbolic tangent curves.

5 Discussion

5.1 Results of the statistical analyses (*t*-test)

The results of the analyses for the statistical significance of the difference between mean values (*t*-test) are summarized in Table 9 (full-size specimens) and Table 10 (sub size specimens) for all the data sets considered, using the same convention described in the legend of Table 2 and including the calculated values of the probability P.

Table 9 Results of the *t*-test for the full-size specimen data sets analyzed in terms of probability and statistical significance (at the 95% confidence level).

Data set	Material	F_{gy}		F_m		s_m		W_t		KV	
		P	Δ	P	Δ	P	Δ	P	Δ	P	Δ
ASTM E28.07	A533B (RT)	0.016	>>	<0.0001	<<<	<0.0001	<<<	0.5487	~	0.4354	~
	A533B (150°C)	<0.0001	>>>	<0.0001	<<<	0.0044	<<	0.6740	~	0.3572	~
	Low E CRM	N/A		0.2105	~	0.0184	<	0.4755	~	0.7835	~
	High E CRM	<0.0001	>>>	0.0547	~	<0.0001	<<<	0.1143	~	0.3136	~
NIST	Low E CRM	N/A		<0.0001	<<<	N/A		0.3223	~	<0.0001	>>>
	High E CRM	<0.0001	<<<	<0.0001	<<<	N/A		<0.0001	>>>	0.4347	~
IAEA CRP8	High E ERM	0.0108	<	0.0409	<	N/A		0.2252	~	0.0030	>>
SCK•CEN	Low E ERM(1)	N/A		0.0010	<<	0.3266	~	0.0567	~	0.0724	~
	Low E ERM(2)	N/A		0.1663	~	<0.0001	<<<	<0.0001	>>>	0.0010	>>
	Medium E ERM	0.3682	~	0.0220	<	0.1413	~	0.6306	~	0.5596	~

Table 10 Results of the *t*-test for the sub size data sets analyzed in terms of probability and statistical significance (at the 95% confidence level).

Data set	Material	F_{gy}		F_m		s_m		W_t		KV	
		P	Δ	P	Δ	P	Δ	P	Δ	P	Δ
ASTM E28.07	A533B (RT)	0.0200	>	<0.0001	<<<	<0.0001	>>>	0.0554	~	N/A	
	A533B (150°C)	0.0010	<<<	<0.0001	<<<	0.0431	>	0.1259	~	0.1596	~
	Low E CRM	N/A		<0.0001	<<<	0.0038	<<	0.0079	<<	N/A	
	High E CRM	0.6422	~	<0.0001	<<<	<0.0001	<<<	0.0168	<	0.4597	~

In order to assess the sensitivity of each parameter to the striking edge configuration, probability values in Tables 9 and 10 were added up and averaged for each variable. When P < 0.0001, P = 0 was assumed in the calculations.

A "striker influence index" (SII) was also defined by replacing the symbols for Δ in Tables 9 and 10 with numbers (> = +1; >> = +2; >>> = +3; < = -1; << = -2; <<< = -3; ~ = 0), and averaging the totals for each variable.

Mean values and SII are given in Table 11 for each variable and specimen type (full-size and sub size). Table 11 should be interpreted as follows:

- the variables with the highest and the lowest mean values $\overline{P}$ are respectively the least and the most sensitive to the influence of striking edge radius;
- for a variable with positive SII, higher values tend to be measured when using a 2mm-striker; the opposite is true if the variable has a negative SII;
- a low absolute value of SII can indicate either a limited sensitivity to the striker configuration or that variations due to striker configuration are not systematic and tend to compensate each other.

Table 11 Sensitivity of the experimental variables to the configuration of the instrumented striker.

		F_{gy}	F_m	s_m	W_t	KV
Full-size specimens	$\overline{P}$	0.066	0.050	0.070	0.305	0.296
	SII	+0.66	-1.60	-1.71	+0.60	+0.70
Sub size specimens	$\overline{P}$	0.221	0.000	0.047	0.052	0.310
	SII	-0.66	-3.00	-0.25	-0.75	0.00

From the examination of Table 11, we observe the following.

(1) For full-size specimens, absorbed energy values (both from the instrumented test record and from the machine encoder) are not very sensitive to the striker configuration, although the values of SII indicate a slightly tendency for higher energy values when using a 2mm-striker. Since none of the examined data sets exceeds 150 J, this is in agreement with the existing literature.

(2) For sub size specimens, the available data is limited and the results in Table 11 should be handled with care. Encoder energy KV and force at general yield F_{gy} have the highest $\overline{P}$; however, the values of SII are significantly different, indicating that KV is indeed insensitive to the striker configuration, whereas a tendency to lower values of F_{gy} for 4mm-strikers is visible from Table 10.

(3) The largest influence for both full-size and sub size specimens is observed on maximum forces F_m and corresponding displacements s_m, with systematically higher values yielded by the 8mm-striker (negative SII values). The effect for s_m, however, is not confirmed by 22NiCrMo37 data measured at SCK•CEN (Fig. 5).

(4) Forces at general yield F_{gy} also appear to be significantly affected, but the general tendency is opposite for full-size (higher values for 2mm-strikers, see also 22NiMoCr37 data in Fig. 3) and sub size[3] (higher values for 4mm-strikers) specimens. Inconsistencies between some data sets can be noted in Tables 9 and 10.

(5) Instrumented absorbed energies for sub size specimens have a low value of $\overline{P}$ and a negative value of SII. This might indicate that the energy level of the available data sets (10-11 J, see Table 3) is close or even beyond the threshold energy for sub size specimens (i.e. equivalent to 200 J for full-size samples).

[3]Again, it must be emphasized that only one round-robin is available for sub size specimens, and this includes only 2 laboratories using a 4mm-striker. More data would be needed to confirm our observations.

5.2 Analytical correlations between 2mm and 8mm-strikers

In an attempt to derive more quantitative relationships for full-size specimens, we have plotted in Fig. 10 to 12 for each of the investigated variables the mean values obtained for the two different strikers. For sub size specimens, not enough data are available to obtain reliable empirical correlations and only qualitative interpretations should be attempted.

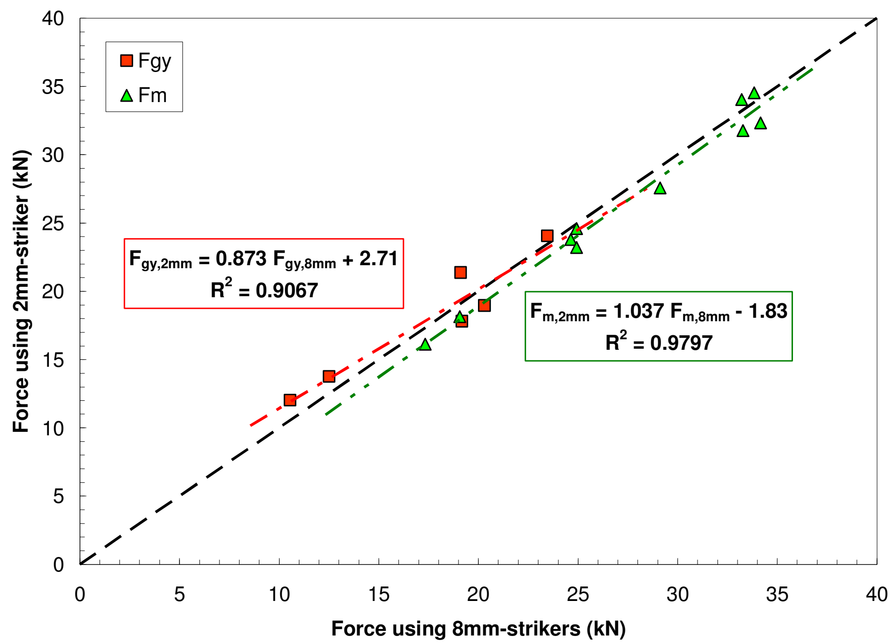

Fig. 10 Correlation between forces at general yield and maximum forces measured with 2mm and 8mm-strikers.

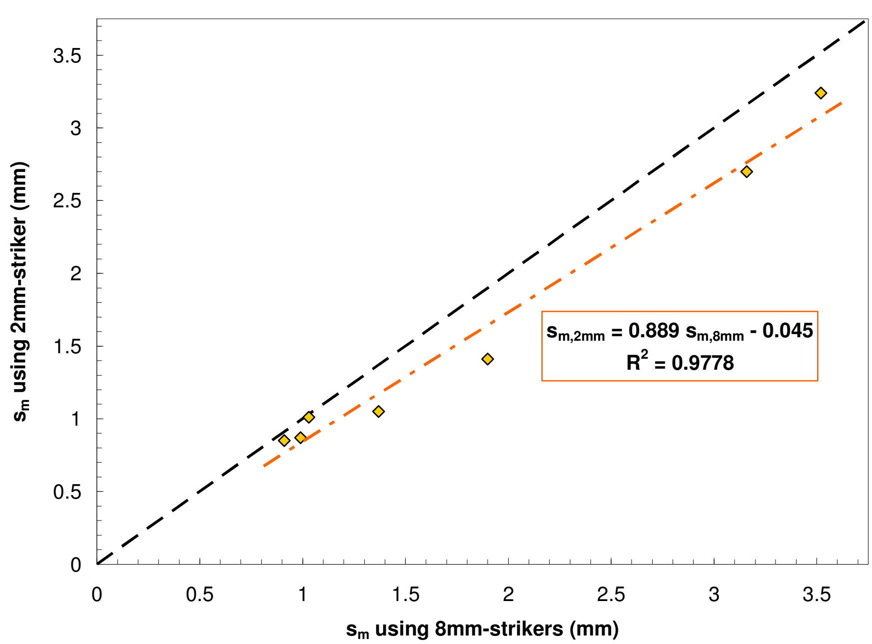

Fig. 11 Correlation between displacements at maximum forces measured with 2mm and 8mm-strikers.

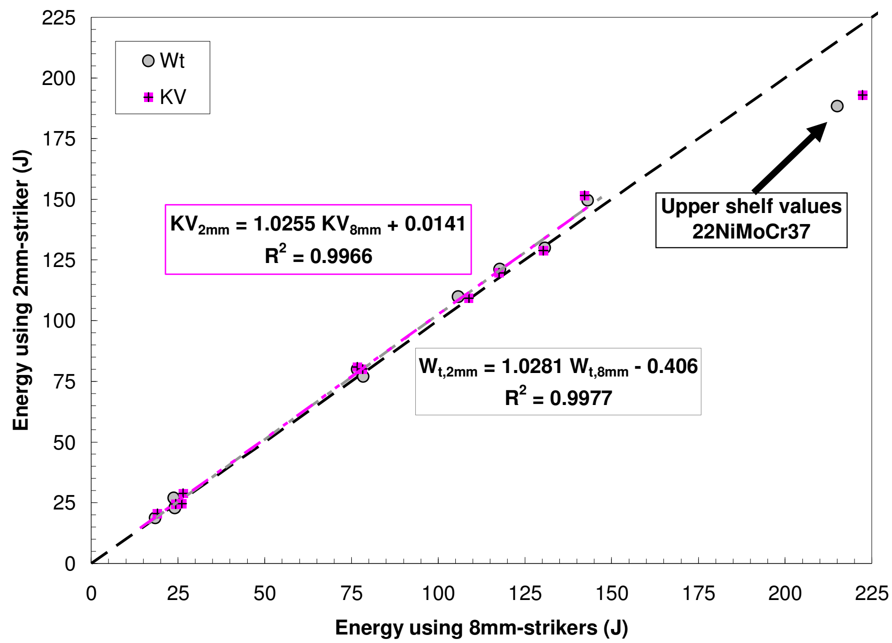

Fig. 12 Correlation between calculated and encoder absorbed energies measured with 2mm and 8mm-strikers, including upper shelf energies measured at SCK•CEN on 22NiMoCr37.

Coefficients of determination (R^2) higher than 0.98 were obtained for all variables except the general yield force. For F_m, s_m, W_t and KV, the slopes of the fitting lines are close to 1 and the intercepts are quite small, indicating that differences between strikers are relatively constant within the investigated ranges.

Once again, the most consistent trends were observed for maximum forces and corresponding displacements.

For absorbed energies, our results are similar to those reported by Fink (Fink 1990), with energies 2-3% higher for 2mm-strikers up to 150 J. Above 200 J, the effect of the interaction between heavily deformed sample and 8mm-striker corners comes into play, as shown by the USE values measured by SCK•CEN on 22NiMoCr37.

The standard errors of estimate for the correlations obtained are: 1.55 kN for F_{gy}, 0.99 kN for F_m, 0.16 mm for s_m, 2.54 J for W_t and 3.08 J for KV.

In order to assess whether our observations are in agreement with the literature, in Fig. 13 we plotted our KV data together with those extracted from the already mentioned literature references, excluding obviously those in which individual data and/or mean values are not tabulated[4].

[4]We are fully aware that the references used represent by no means an exhaustive review of the existing literature. Nevertheless, we believe they represent a meaningful sample of the existing data.

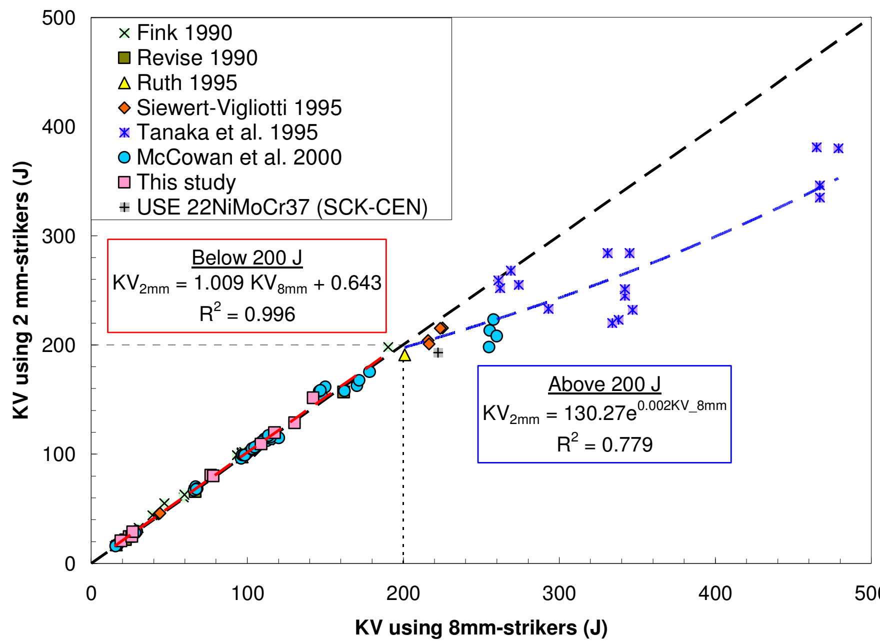

Fig. 13 Correlation between encoder absorbed energies measured with 2mm and 8mm-strikers, using data from this study and from several literature references.

The database represented in Fig. 13 consists of 111 data points, each one corresponding to the mean value for a series of Charpy tests. 77% of the points are below 200 J. The Figure also includes the USE values measured at SCK•CEN on 22NiMoCr37; this point was not used for the obtainment of the regression curves.

Below a threshold value which we have arbitrarily (but reasonably) set at 200 J, energies measured from both strikers are in close agreement, with a value only marginally higher (by less than 1%) for 2mm-strikers. The degree of linear correlation is very significant ($R^2 = 0.996$) and the standard error of the estimate is 3.29 J.

Above 200 J, more scatter is observed, but it's clear that the 8mm-striker gives higher absorbed energies, due to the interaction between the plastically deformed samples and the corners of the striker. We have arbitrarily chosen a power law for fitting data above 200 J, which yields a good coefficient of determination ($R^2 = 0.779$); other fitting functions would have given equally acceptable results.

The results analyzed in this study, including upper shelf energies for 22NiMoCr37, are in agreement with the available literature.

5.3 Influence of material toughness

Finally, we have plotted the data as a function of absorbed energy, which can be used as an index of material toughness or ductility. The ratio between mean values obtained from 2mm and 8mm-strikers is shown as a function of average[5] KV for forces (Fig. 14), s_m (Fig. 15) and energies (Fig. 16). These data can be compared with SCK•CEN results on 22NiMoCr37 in Figs. 3 to 7, where test temperature can also be adopted as an index of material toughness.

[5] Average value between KV measured with 2mm and 8mm-strikers.

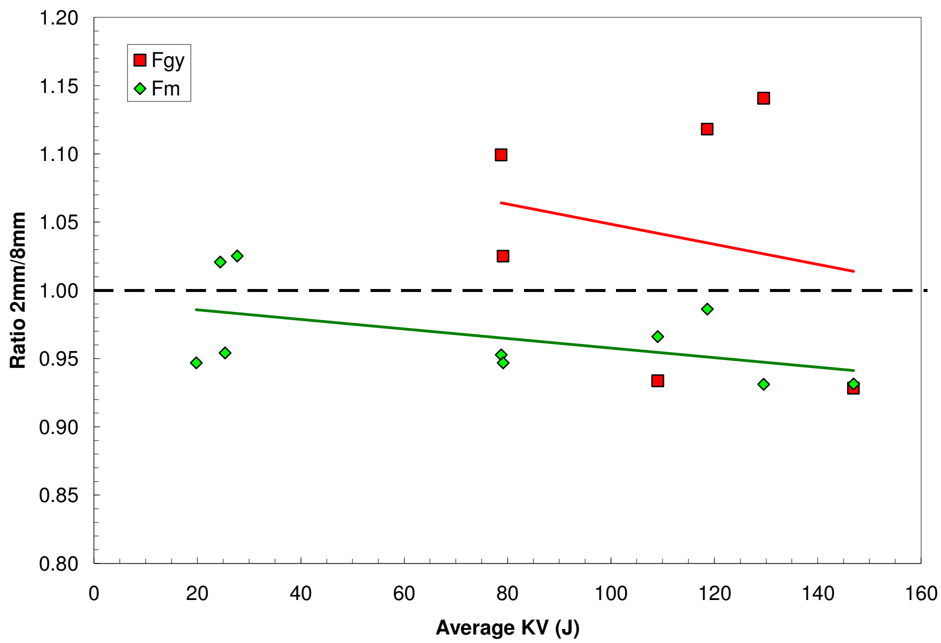

Fig. 14 2mm/8mm ratio as a function of absorbed energy for forces at general yield and maximum forces.

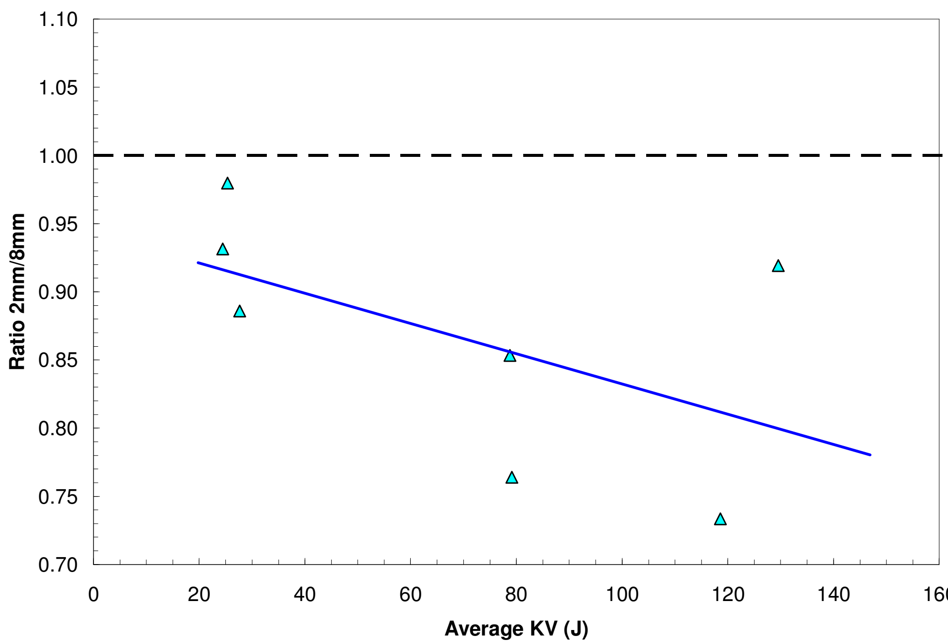

Fig. 15 2mm/8mm ratio as a function of absorbed energy for displacement at maximum force.

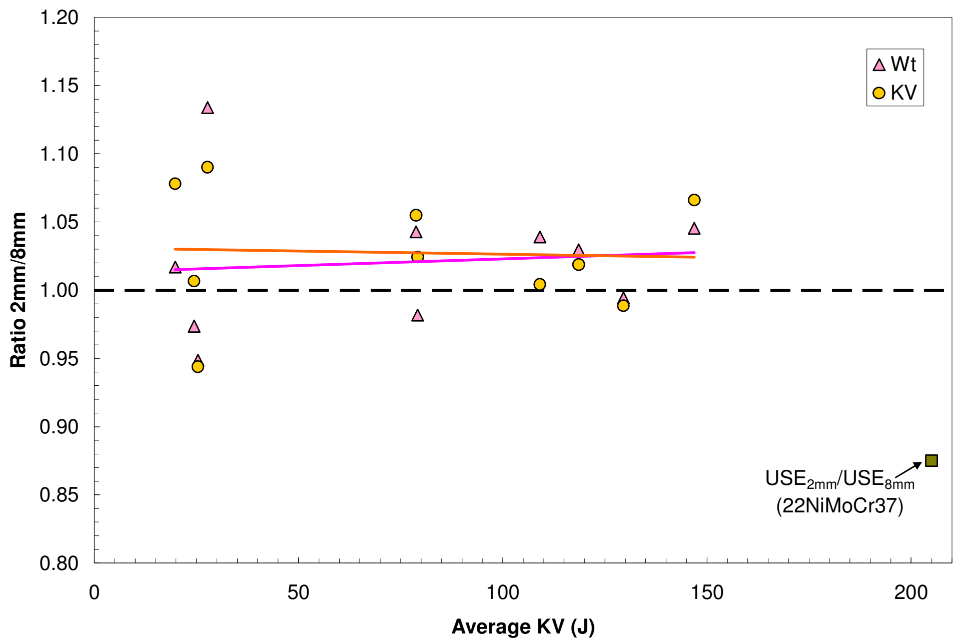

Fig. 16 2mm/8mm ratio as a function of absorbed energy for calculated and encoder energies.

Despite the experimental scatter, we observe that the influence of striking edge radius on forces and displacements (Figs. 14 and 15) tends to increase with increasing material toughness, with the 8mm-striker delivering progressively higher results as the sample becomes more ductile. This is confirmed by Figs. 3 and 4, where 2mm-striker values are consistently higher for F_{gy} and lower for F_m across the whole range of material behavior from fully brittle (low temperatures) to fully ductile (high temperatures).

Absorbed energies appear less sensitive to impact toughness and no clear trend can be identified up to 150 J (Fig. 16). The results obtained at SCK•CEN on 22NiMoCr37 (Figs. 6 and 7) indicate that the situation changes significantly at higher toughness levels. The divergence between 22NiMoCr37 transition curves occurs around 40-50 J, which is in broad agreement with the value of 60 J (0.75 J/mm²) reported in (Morita and Kobayashi 2004) for A508 cl.3 steel.

5.4 Influence of striker configuration on data scatter

Siewert and Vigliotti (Siewert and Vigliotti, 1995) addressed the influence of striker configuration on the scatter of absorbed energy results, i.e. on the standard deviation of KV data measured with 2mm and 8mm-strikers. We performed a similar analysis, including also characteristic forces, displacements and energies measured from the instrumented traces.

In Fig. 17, relative standard deviations (in % with respect to the mean values) for the two striker configurations are plotted, using data from this investigation and from the same references used in Fig 13, except for one (Revise, 1990) which does not report standard deviations. Considerable scatter is observed, but a general tendency can be noted for higher standard deviations when using 2mm-strikers. However, closer examination of Fig. 17 reveals that this effect is practically negligible for F_{gy}, F_m and KV and more significant for s_m and W_t.

Fig. 18 shows the ratio between standard deviations measured with 2mm and 8mm-strikers as a function of average absorbed energy KV (defined as previously for Figs.14-16). The overall trend, indicated by the red dotted line, shows a general increase of the standard deviation for 2mm-strikers with increasing material toughness/ductility. However, below 200 J (green solid line), no clear influence of KV is detected.

Our observations are substantially consistent with those in (Siewert and Vigliotti, 1995), who reported for the 2mm-striker standard deviations at 200 J about 3 times as large as those for the 8mm-striker.

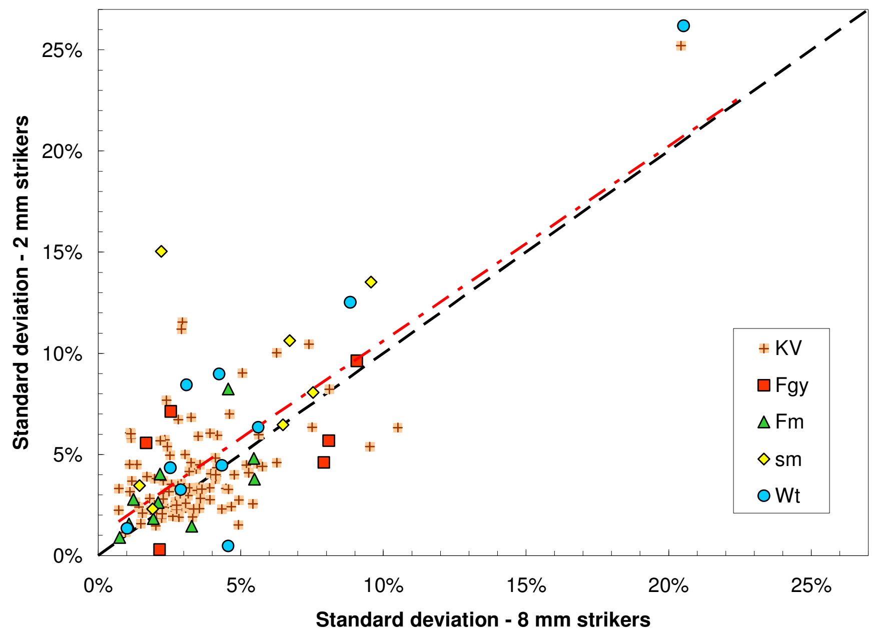

Fig. 17 Relationship between standard deviations for 2mm and 8mm-strikers.

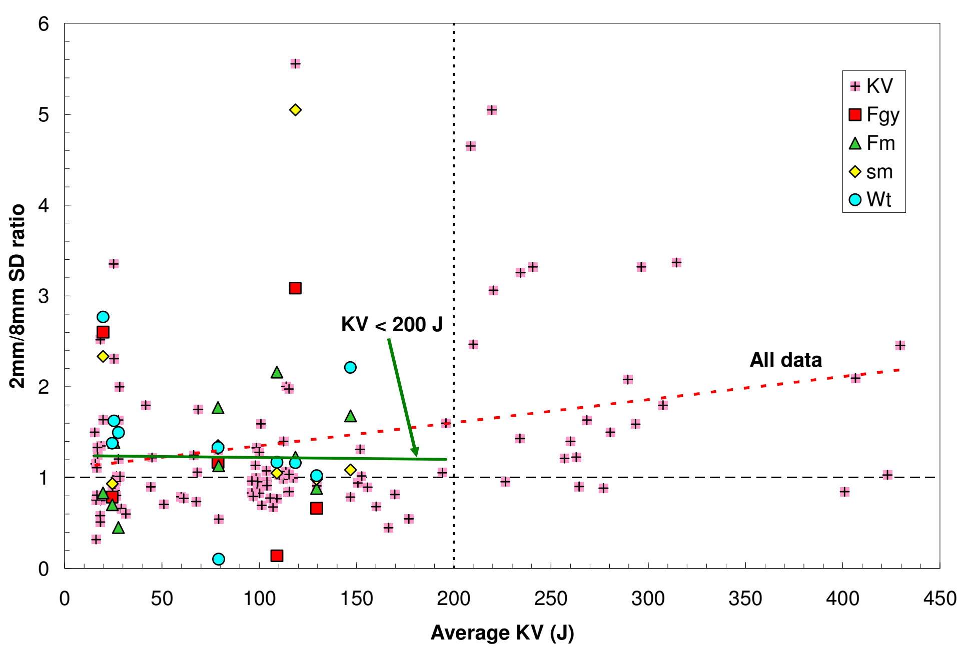

Fig. 18 Ratio between standard deviations as a function of material toughness.

6 Conclusions

The results of three interlaboratory studies on instrumented Charpy tests of full-size and sub size Charpy specimens were analyzed in order to investigate the influence of the striking edge radius (2 mm or 8 mm) on characteristic values of force, displacement and energy. In addition, results obtained at SCK•CEN by testing the same materials on the same machines with different strikers were also examined.

The main findings for full-size specimens are summarized below.

(a) Forces at general yield (F_{gy}) are certainly affected by striker configuration, but the effect is not systematic and significant scatter is observed. Generally, F_{gy} values from 2mm-strikers tend to be higher, but the difference seems to decrease with material toughness.

(b) Maximum forces (F_m) and corresponding displacements (s_m) show the most significant effect of striker configuration, with 8mm-strikers providing consistently higher values. The effect increases with material toughness.

(c) Absorbed energies measured from the instrumented traces (W_t) and from the machine encoder (KV) behave very similarly. Below 200 J, striker effect is marginal (no more than a few %). Above 200 J, 8mm-strikers deliver progressively higher absorbed energy, due to the interaction between heavily deformed specimen and the sharp corners of the 8mm-striker and the increased sample/anvils friction, that cause additional energy consumption.

(d) Data scatter is generally higher for 2mm-strikers than for 8mm-strikers.

(e) The results presented in this study are consistent with the existing literature.

For sub size specimens, only one interlaboratory study was examined, with only two labs using a 4mm-striker and the rest using 2mm-strikers. The following indications, which should be confirmed by additional testing, have emerged.

(a) The effect on F_m and s_m is consistent with that observed for full-size specimens (higher values for the larger striking edge radius).

(b) The effect on F_{gy} is unclear.

(c) In the narrow range investigated (10-11 J), absorbed energies W_t and KV do not show large sensitivity to the striker configuration.

No analytical correlation was derived for sub size specimens, on account of the limited available data base.

References

ASTM International (2000) Pendulum Impact Testing: A Century of Progress. ASTM STP 1380. Siewert TA and Manahan MP, editors

ESIS (2002) From Charpy to Present Impact Testing. Proceedings of the Charpy Centenary Conference, CCC2001, Poitiers (France), 2-5 October 2001. ESIS Publication 30. François D, Pineau A, editors. Elsevier, Amsterdam

Fink DA (1990) Quantitative Comparison and Evaluation of Various Notch Machining Methods and How They Affect ASTM E23 and ISO R442 Testing Equipment Results. In: Charpy Impact Test: Factors and Variables. ASTM STP 1072. American Society for Testing and Materials, Philadelphia 94-119

Heerens J, Hellmann D (2002) Development of the Euro Fracture Toughness Dataset. Eng Fract Mech 69(4):421-449

Kang KS (2007) IAEA Coordinated Research Projects on Master Curve Technology: An Overview. In: Proceedings of 2007 Pressure Vessels & Piping Conference and The Eighth International Conference on Creep and Fatigue at Elevated Temperatures, ASME PVP 2007/CREEP 8, San Antonio TX 22-26 July 2007. Paper PVP2007-26351

Lucon E, Viehrig H-W (2007) Round-Robin Exercise on Instrumented Impact Testing of Precracked Charpy Specimens (IAEA Coordinated Research Program Phase 8). In: Proceedings of 2007 Pressure Vessels & Piping Conference and The Eighth International Conference on Creep and Fatigue at Elevated Temperatures, ASME PVP 2007/CREEP 8, San Antonio TX 22-26 July 2007. Paper PVP2007-26088

Manahan MP, Martin FJ, Stonesifer RB (2000) Results of the ASTM Instrumented/Miniaturized Round Robin Test Program. In: Pendulum Impact Testing: A Century of Progress. ASTM STP 1380. ASTM International, West Conshohocken PA 223-241

McCowan CN, Pauwels J, Revise G, Nakano H (2000) International Comparison of Impact Verification Programs. In: Pendulum Impact Testing: A Century of Progress. ASTM STP 1380. ASTM International, West Conshohocken PA 73-89

McCowan CN, Splett JD, Lucon E (2008) Dynamic Force Measurement: Instrumented Charpy Impact Testing. NISTIR 6652, National Institute of Standards and Technology, Boulder CO

Morita S, Kobayashi T (2004) Ductile-Brittle Transition Behaviors with Two Striker Geometries in the Instrumented Charpy Impact Test. Mat Sc Forum 449-452:861-864

Naniwa T, Shibaike M, Tanaka M, Tani H, Shiota K, Namio H, Shiraishi T (1990) Effects of the Striking Edge Radius on the Charpy Impact Test. In: Charpy Impact Test: Factors and Variables. ASTM STP 1072. American Society for Testing and Materials, Philadelphia 67-80

Nanstad RK, Sokolov MA (1995) Charpy Impact Test Results on Five Materials and NIST Verification Specimens Using Instrumented 2-mm and 8-mm Strikers. In: Pendulum Impact Machines: Procedures and Specimens for Verification. ASTM STP 1248. American Society for Testing and Materials, Philadelphia 111-139

Revise G (1990) Influence of Dimensional Parameter of an Impact Test Machine on the Results of a Test. In: Charpy Impact Test: Factors and Variables. ASTM STP 1072. American Society for Testing and Materials, Philadelphia 35-53

Ruth EA (1995) Striker Geometry and Its Effect on Absorbed Energy. In: Pendulum Impact Machines: Procedures and Specimens for Verification. ASTM STP 1248. American Society for Testing and Materials, Philadelphia 101-110

Schuurmans J, Scibetta M, Lucon E, Puzzolante J-L (2008) Influence of Strain Gage Position on the Static and Dynamic Performance of Instrumented Impact Strikers. J of Test and Eval (submitted)

Siewert TA, Manahan MP, McCowan CN, Holt JM, Marsh FJ, Ruth EA (2000) The History and Importance of Impact Testing. In: Pendulum Impact Testing: A Century of Progress. ASTM STP 1380. ASTM International, West Conshohocken PA 3-16

Siewert TA, Vigliotti DP (1995) The Effect of Charpy V-Notch Striker Radii on the Absorbed Energy. In: Pendulum Impact Machines: Procedures and Specimens for Verification. ASTM STP 1248. American Society for Testing and Materials, Philadelphia 140-152

Tanaka M, Ohno Y, Horigome H, Tani H, Shiota K, Misawa A (1995) Effects of the Striking Edge Radius and Asymmetrical Strikes on Charpy Impact Test Results. In: Pendulum Impact Machines: Procedures and Specimens for Verification. ASTM STP 1248. American Society for Testing and Materials, Philadelphia 153-167

Towers OL (1983) Effects of Striker Geometry on Charpy Results. Met Constr 15(11):682-686

Viehrig H-W and Lucon E (2007) IAEA Coordinated Research Project on Master Curve Approach to Monitor Fracture Toughness of RPV Steels: Effect of Loading Rate. In: Proceedings of 2007 Pressure Vessels & Piping Conference and The Eighth International

Conference on Creep and Fatigue at Elevated Temperatures, ASME PVP 2007/CREEP 8, San Antonio TX 22-26 July 2007. Paper PVP2007-26087